Preprints of the 21st IFAC World Congress (Virtual)
Berlin, Germany, July 12-17, 2020

Grid and Polytopic LPV Modeling of Aeroelastic Aircraft for Co-design

Réka Dóra Mocsányi, * **Béla Takarics,** * **Bálint Vanek** *

* *Institute for Computer Science and Control, Kende u. 13-17., 1111 Budapest, Hungary (e-mail: {mocsnyi, takarics, vanek}@sztaki.hu).*

Abstract: Future aircraft tend to have increased flexibility that leads to increased aeroservoelastic (ASE) effects. Therefore, future aircraft control systems need active control to suppress ASE effects. Active flutter suppression can be effectively done in the linear parameter varying (LPV) framework. Control surface sizing for aircraft is traditionally done by iterations. In this approach engineering rules are used to determine the size of the control surfaces and the control laws are designed afterwards. Such method, besides being time consuming, might have further challenges in the future due to the coupling between the flexible and rigid body dynamics. Instead, "co-design" was recently proposed. In the co-design approach parametric aircraft models are developed based on which the control surface sizing and the control design are optimized in a single step. The purpose of this paper is to create a control oriented, parametric control surface model of the mini MUTT aircraft that can be applied for co-design. The resulting control oriented LPV model needs to have sufficiently low dynamic order, which is achieved by the "bottom-up" modeling approach. A grid based LPV model is obtained from the nonlinear model by Jacobian linearization and the Tensor Product (TP) type polytopic model is obtained from the grid based LPV model via TP model transformation. The resulting low order parametric control surface LPV models are assessed with the ν-gap metric. These models can serve as the basis of simultaneous baseline/flutter suppression control synthesis and control surface sizing optimization.

Keywords: Parameter-varying systems, Aeroelasticity, UAVs, Model reduction

1. INTRODUCTION

Future aircraft tend to have increased flexibility that leads to increased aeroservoelastic (ASE) effects. There are several recent projects in the USA and EU dealing with aeroservoelastic aircraft and active flutter suppression (PAAW (2014-2019); FLEXOP (2015-2019); FliPASED (2019-2022)). Controllability of a flight vehicle depends on a number of factors, including the geometry of control surfaces. In return, options and limitations of control design influence the geometry as well. Therefore, control surface sizing is a critical task in flexible aircraft design. The classical concept of aircraft design places a great emphasis on engineering rules. Initially, geometric sizing is defined based on these rules, then control laws are synthesized for the resulting construction. In case of incompatibility between the designed geometry and control laws, the sizing is changed according to the existing control law, and then control laws are redesigned for the new geometry (Denieul et al. (2017)). In case of aeroelastic aircraft such classical approach might no longer be valid due to the coupling between flexible dynamics and rigid body dynamics. Thus, sizing demands the consideration of control laws at and early stage of the design process. Therefore, instead of the iterative control design method, a new approach can be applied called Co-design (Denieul et al. (2017)). In addition to engineering rules it takes limitations of control laws into consideration. Thus, control surface sizing and control design can be optimized in a single step. A new variable (μ) is introduced to parameterize the control surface size. The aim of the co-design approach is to determine the optimal control law and control surface size. The key idea is to integrate the parametric aircraft model into the control design problem as presented in Figure 1. A Linear Fractional Representation (LFR) can be used for such integration (Denieul et al. (2017)).

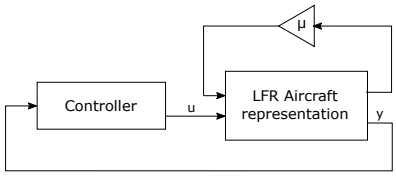

Fig. 1. Integrated design and control optimization.

A suitable control oriented aeroservoelastic (ASE) model is required to carry out simultaneous flutter suppression control design and control surface sizing (Theis et al. (2016); Schmidt et al. (2019)). The linear parameter-varying (LPV) framework (Shamma (1988), Section 2.) is a typical approach to model ASE systems suitably for control design. The specific flexible aircraft considered in this paper is the Mini MUTT (Multi Utility Technology Testbed) flying wing (Section 3.), an unmanned flying wing built by the UAV Lab at the University of Minnesota (PAAW (2014-2019)). The mini MUTT aircraft can be parameterized by control surface properties (Section 4.). A

nonlinear ASE model is built (Section 5.) applying a subsystem based approach. Subsystems blocks representing flight dynamics, aerodynamics and structural dynamics are constructed individually and later combined in the ASE model. However, the resulting ASE models (high fidelity) in general are of high dimension and their reduction propose quite a challenge. Thus, "bottom-up" modeling (Takarics et al. (2018)) is used to generate lower order (low fidelity) system representations (Section 6.). The assessment of the "bottom-up" model is done with grid-based LPV models. In addition to the grid-based low order LPV models (Wu (1995)), TP type (Baranyi et al. (2013)) polytopic LPV models are generated. The grid-based and TP type polytopic LPV models complement each other and both can be used for co-design. The modeling process is presented in Figure 2.

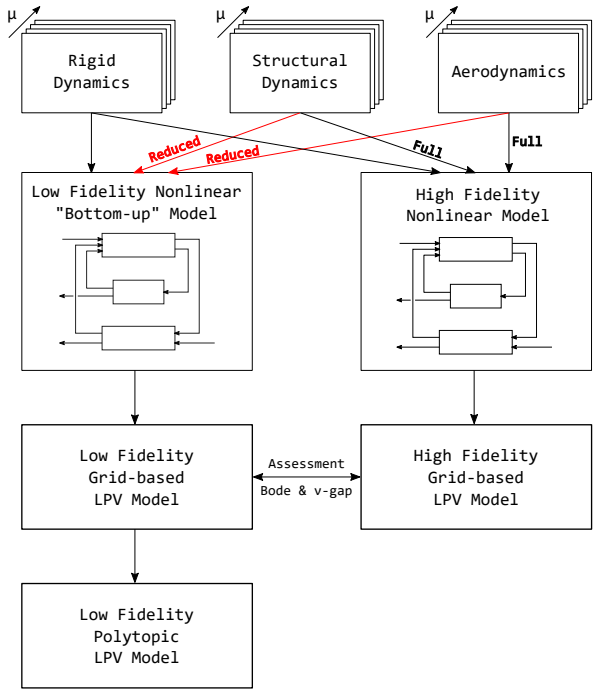

Fig. 2. ASE modeling and assessment process.

2. LPV FRAMEWORK

An LPV system can be described by the state space model (Shamma (1988))

$$\begin{aligned} \dot{x} &= A(\rho)x + B(\rho)u \\ y &= C(\rho)x + D(\rho)u \end{aligned} \tag{1}$$

with the continuous matrix functions $A\colon \mathcal{P} \to \mathbb{R}^{n_x \times n_x}$, $B\colon \mathcal{P} \to \mathbb{R}^{n_x \times n_u}$, $C\colon \mathcal{P} \to \mathbb{R}^{n_y \times n_x}$, $D\colon \mathcal{P} \to \mathbb{R}^{n_y \times n_u}$, the state $x\colon \mathbb{R} \to \mathbb{R}^{n_x}$, input $u\colon \mathbb{R} \to \mathbb{R}^{n_u}$, output $y\colon \mathbb{R} \to \mathbb{R}^{n_y}$ and a time-varying scheduling signal $\rho : \mathbb{R} \to \mathcal{P}$, where $\mathcal{P}$ is a compact subset of $\mathbb{R}^{\rho}$.

Different types of representations are available for LPV systems, including grid-based (Wu (1995)), linear fractional transformation (LFT) (Packard (1994); Veenman and Scherer (2013)) and polytopic (Apkarian et al. (1995)) approaches. In this case the grid-based and polytopic approaches are investigated. In a grid representation, an LPV system is defined as a set of LTI models $(A_k, B_k, C_k, D_k) = (A(\rho_k), B(\rho_k), C(\rho_k), D(\rho_k))$ obtained from evaluating the LPV model at a finite number of parameter values $\rho_{k1}^{N_grid} = \mathcal{P}_grid \in \mathcal{P}$. In this case the system is stored on a finite gridded domain as a state-space array. To compute a sufficiently accurate model the grid must be dense enough, which can lead to high computational cost at the control synthesis. Polytopic model representation can mitigate the computational cost of grid-based LPV models at the expense of more conservative results. Let the system matrix be written as

$$S(\rho(t)) = \begin{pmatrix} A(\rho(t))B(\rho(t)) \\ C(\rho(t))D(\rho(t)) \end{pmatrix} \tag{2}$$

The dependence on time t is occasionally suppressed in the remainder of the paper to shorten the notation. The system matrix $S(\rho)$ of (2) is reconstructed for any parameter ρ with the following polytopic structure:

$$S(\rho) = \sum_{r=1}^{R} w_r(\rho) S_r \tag{3}$$

The ordering $r = ordering(i_1, i_2, \dots i_N)$, determines r as a linear index of the multilinear array index of the size $I_1 \times I_2 \dots I_N$, $w_r(\rho) = \prod_{n=1}^{N} w_{n,i_n}(\rho_n(t))$ and $S_r = S_{i_1,\dots,i_N}$. The canonical HOSVD based polytopic TP model form of (3) consists of (Baranyi et al. (2013)):

$$S(\rho) = \sum_{i_1=1}^{I_1} \cdots \sum_{i_N=1}^{I_N} \prod_{n=1}^{N} w_{n,i_n}(\rho_n) S_{i_1,\dots,i_N} \tag{4}$$

which consists of weighting functions $w_n(\rho_n(t))$ and the parameter varying, singular value ordered orthonormal combination of Linear Time-Invariant (LTI) matrices $S \in \mathbb{R}^{O \times I}$ (termed as vertexes). With the compact tensor notation the canonical HOSVD based polytopic TP model form (4) results in:

$$S(\rho) = \mathcal{S} \underset{n \in N}{\boxtimes} w_n(\rho_n) \tag{5}$$

The core tensor's coefficients $\mathcal{S} \in \mathbb{R}^{I_1 \times \dots \times I_N \times O \times I}$ are constructed from the LTI vertex matrices $S_{i_1,\dots,i_N}$, row vectors $w_n(\rho_n)$ from the univariate weighting functions $w_{n,i_n}(\rho_n)$, $i_n = 1 \dots I_N$ and ρ_n consists of the n-th element of vector ρ. A convex TP model representation can be obtained from a grid-based LPV model via TP model transformation (Baranyi et al. (2013)).

3. THE MINI MUTT AIRCRAFT

The aircraft considered in this paper is shown in Figure 3. The Mini MUTT's design (Regan and Taylor (2016); PAAW (2014-2019)) is based on the BFF aircraft (Air Force Research Laboratory and Lockheed Martin (LM)) and the X-56 MUTT aircraft (LM). The geometry contains eight flaps, built in for various purposes. The flaps marked with green - two on the body and the two outer ones on the wing - are for flutter suppression. The blue colored control surfaces are used as ailerons driven differentially and the orange colored ones are the elevators that are driven together. The aircraft has gyros at the center of gravity (CG), rate and acceleration sensors in the wing as shown in Figure 3. All data related to ground tests, flight tests, the aerodynamic design of the aircraft, aerodynamics modeling software and control design tools are open to the public (AEM ASE (2013)).

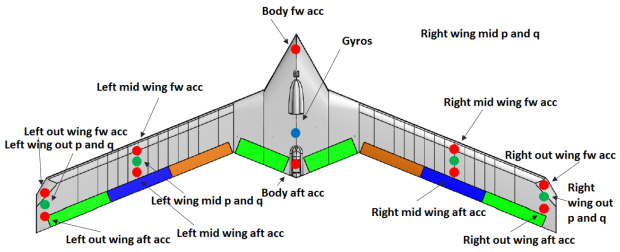

Fig. 3. Mini MUTT aircraft.

4. CO-DESIGN CONSIDERATIONS

In this section a new approach to control surface sizing based on (Denieul et al. (2017)) is described. Applying this method, control surface sizing and flutter control design can be optimized in a single step. For this, a set of parametric models is required that is available early in the aircraft design stage. A new variable μ is introduced to capture the parametric variation of the model. μ can capture several parameters of the aircraft. However, an overly increased set of parameters leads to very complex parametric models which might not be suitable for co-design. In the present case, μ captures the control surface geometry. The parameter value $\mu = 1$ belongs to the initial layout of the control surfaces. The chosen varying parameters for the co-design of the Mini MUTT are the chord length of the control surfaces and the weight of the actuators. A range of discrete values of $\mu \in [0.75\ 1.25]$ is selected, see Figure 4. In this case only one of the chosen parameters is independent. Two versions with extended chords and heavier actuators and two versions with decreased chord length and lighter actuators are created. To maintain clarity the original layout is called 'reference' aircraft. The

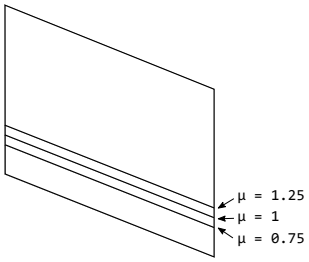

Fig. 4. Wing section parameterized by μ.

main goal of parametric control surface design, or co-design is to expand the aircraft design process with the control design problem. This is achieved by creating a set of continuously parametrized state-space representations. Parametrization can be achieved by computing separate aerodynamic models for a set of discrete μ values. Finally, after obtaining the corresponding aerodynamic coefficients for each model using an appropriate software, a function fitting is carried out on these coefficients. For simplicity, a linear relationship between the chord length of the control surfaces and the actuator weights is assumed. μ values and the corresponding control surface chords, actuator masses and CG positions are presented in Table 1. c_{f_w} and c_{f_b} represent wing flap and body flap chord lengths respectively. The CG also becomes parametric, due to the modification of several equipment masses. With increasing actuator weight the CG shifts towards the trailing edge,

Table 1. Parametric chord lengths and actuator masses.

μ	c_{f_w} $[mm]$	c_{f_b} $[mm]$	m_{act} (1,4) $[g]$	m_{act} (2,3) $[g]$	CG $[mm]$
0.75	72	51.75	48.75	15	577.10
0.875	84	60.375	56.875	17.5	578.07
1	96	69	65	20	579.02
1.125	108	77.625	73.125	22.5	579.95
1.25	120	86.25	81.25	25	580.87

as most of the servos are situated behind the reference aircraft's CG position. The final objective is to define a parametric model suitable for co-design. In this case, μ and the flutter suppression controllers can be simultaneously optimized in the co-design framework.

5. PARAMETRIC AEROELASTIC AIRCRAFT MODELING

The subsystem based nonlinear model of a flexible aircraft is shown in Figure 5. Adopting this approach, the subsystems representing aerodynamics, flight dynamics and structural dynamics are developed individually. The overall aeroelastic model is obtained by combining these subsystems. Advantages of this approach is that different modeling techniques can be applied to different subsystems and their fine-tuning, the models can be updated with test data and additional models such as sensor dynamics can be easily added in order to achieve the overall ASE model.

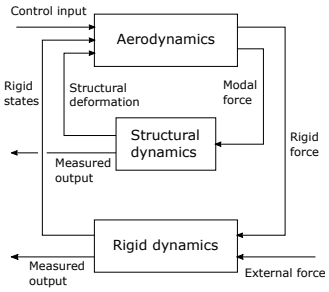

Fig. 5. Subsystem interconnection.

5.1 Numerical modeling tools

The unsteady aerodynamics model is derived via the Matlab toolbox DLMTools and the structural dynamics via FEMCode. These tools are developed by the UMN research group (Kotikalpudi (2017)). In addition, XFLR5 software (Deperrois (2019)) is used to obtain additional aerodynamic coefficients and derivatives.

5.2 High fidelity, parametric ASE model of the mini MUTT

Detailed description of the ASE modeling of Mini MUTT can be found in (Kotikalpudi (2017); Takarics et al.

(2018)). Here only a brief overview is presented with a special emphasis on making the ASE model parametric. The nonlinear equations of motion are obtained in a mean axes reference coordinate frame (Schmidt (2011)) and simplify as

$$\begin{bmatrix} m(\mu)I & 0 \\ 0 & J_{\text{rig}}(\mu) \end{bmatrix} \begin{bmatrix} \dot{V}_{\text{r}} \\ \dot{\Omega}_{\text{r}} \end{bmatrix} + \begin{bmatrix} m(\mu)I\Omega_{\text{r}} \times V_{\text{r}} \\ \Omega_{\text{r}} \times J_{\text{rig}}(\mu)\Omega_{\text{r}} \end{bmatrix} = \begin{bmatrix} \sum F_i \\ \sum M_i \end{bmatrix} \quad (6)$$

where m and J_{rig} are the mass and rigid inertia of the aircraft, and are parameterized by μ. V_{r} and Ω_{r} the translational and angular velocities in the mean axes frame with respect to inertial axes and F_i and M_i are the forces and moments along the mean axes.

Structural dynamics model The structural model of the aircraft is created by applying the finite element method. The linear finite element model is made up of Euler-Bernoulli beams with added torsional effects. Point masses represent payloads and avionics. The beams are connected with nodes that have 3 degrees of freedom each, specifically heaving, twisting and bending. The structural model is parametrized by assuming a simple linear relationship between the control surface chord lengths and the actuator weights. It should be noted, that the chosen method can be replaced by a more complex and accurate connection regarding the control surface size and actuator weight.

Unsteady aerodynamics model Unsteady aerodynamics is modeled applying the subsonic doublet lattice method (DLM) while substituting the solution of the vortex lattice method (VLM) for steady flow obtained at zero oscillating frequency. Both of the methods are potential-based panel methods. These require a lifting surface that is separated into a grid of panels. The DLMTools toolbox generates the Aerodynamic Influence Coefficient (AIC) matrix for the generated aerodynamic grid, from which the Generalized Aerodynamic Matrix (GAM) can be computed. The resulting GAM matrices are computed only over a discrete reduced frequency grid. However, this discrete model is not suitable for time domain aeroelastic simulations. Therefore, a continuous model has to be generated, in this case using Roger's rational function approximation (RFA) method (L. Roger (1977)). Using RFA, additional lag states are included representing the lag behaviour of the aerodynamic model. The grid of the aerodynamics model is parameterized by μ. The chord lengths of the control surfaces are different for each model, but the number of chordwise divisions on the wing and the flaps remain unchanged. This is due to the fact that the thumb rules of grid setup for the chosen μ values do not allow any modification.

Since the resulting aircraft representation only accounts for three force and moment components due to the degrees of freedom of the chosen beam type, the remaining aerodynamic forces and moments are obtained from rigid body aerodynamics coefficients derived by XFLR5. Combining the parameterized rigid body dynamics, structural dynamics and aerodynamics results in the parametric, high fidelity, nonlinear ASE model of the mini MUTT aircraft.

6. PARAMETRIC BOTTOM-UP MODEL OF THE MINI MUTT AIRCRAFT

The high fidelity, nonlinear, parametric model of the Mini MUTT, derived in the previous section, has 12 elastic states with a 52 state aerodynamic model. This nonlinear ASE aircraft model is of too high dimension for control synthesis and implementation. Therefore model order reduction is required to achieve a control oriented model. A "bottom-up" modeling approach, as presented in (Takarics et al. (2018)), is pursued. The main idea of the reduction is the following. The ASE model built from the FEM and DLM based subsystems has a simpler structure than the combined ASE model. With this in mind, order-reduction of the model components can be achieved by using simpler reduction techniques with more tractability. The key considerations when building the low order subsystems are the following. To determine the modes that can be effectively controlled, the actuator bandwidth of the ASE aircraft is used. The frequency range of interest is defined up to 100 rad/s. This range is wide enough to capture the flutter mode, which is at 26.5 rad/s, while the actuator bandwidth of the mini MUTT aircraft is 133 rad/s. Based on these considerations, from the structural modes only the first 4 stand within the frequency region of interest, specifically the 1^{st} symmetric and anti-symmetric bending and torsion modes. The remaining modes are truncated from the linear structural dynamics model resulting in 4 elastic states. In case of the unsteady aerodynamics model, the GAM matrices are generated based on the retained 4 elastic modes resulting in 36 lag states. A linear balancing transformation is used to reduce the parametric unsteady aerodynamic mode and only 4 states corresponding to the highest Hankel singular values are retained. Combining these reduced order subsystems results in the parametric, low fidelity "bottom-up", nonlinear ASE model of the Mini MUTT aircraft. The order of this model is sufficiently low for control synthesis.

6.1 Grid-based low fidelity LPV model of the mini MUTT

In the next step, the accuracy of the "bottom-up" model needs to be assessed. A way to compare the high and low fidelity nonlinear ASE models are time domain simulations. In the present case, linear analysis tools are used for the assessment. First, a grid-based LPV model is constructed from the high and low fidelity ASE models. The grid-based model can be generated for the Mini MUTT by Jacobian linearization as given in (Takarics and Seiler (2015)). Trimming of the aircraft dynamics is executed in straight and level flight condition with the airspeed range at $V = [20, 33]\ m/s$ at 27 equidistant points. Thus the airspeed becomes a scheduling parameter ρ. In addition, μ is treated as an additional scheduling variable which has zero bounds on its rate. The resulting model is defined on a grid of size 27×5.

The main measure to compare the original full-order and the bottom-up model of the aircraft is the ν-gap metric, (Vinnicombe (1993)). It takes values between zero and one, where zero is attained for two identical systems. It can be observed from Figure 6. that the ν-gap values are low for up to 90 rad/s frequency and grow rapidly above

100 rad/s. Therefore, the accuracy of the low fidelity LPV model is sufficient within the frequency range of interest.

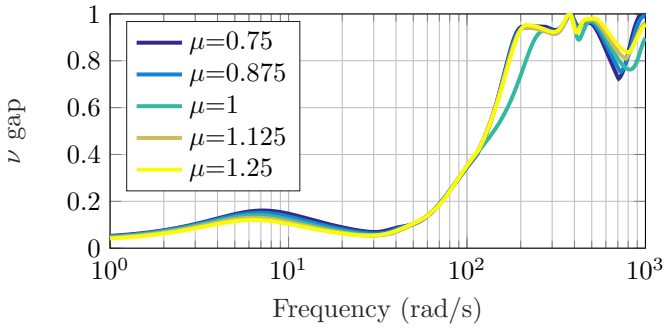

Fig. 6. ν-gap metrics of the low and high fidelity models.

As an additional assessment, the Bode plots of the low and high fidelity parametric models at airspeed close to the flutter speed are compared in Figure 7. The figures show good matching between the high and low fidelity models in the frequency range of interest and that there is a difference in the gains when the different μ values are considered. A flutter peak can be observed at 26.5 rad/s frequency at $V = 25$ m/s.

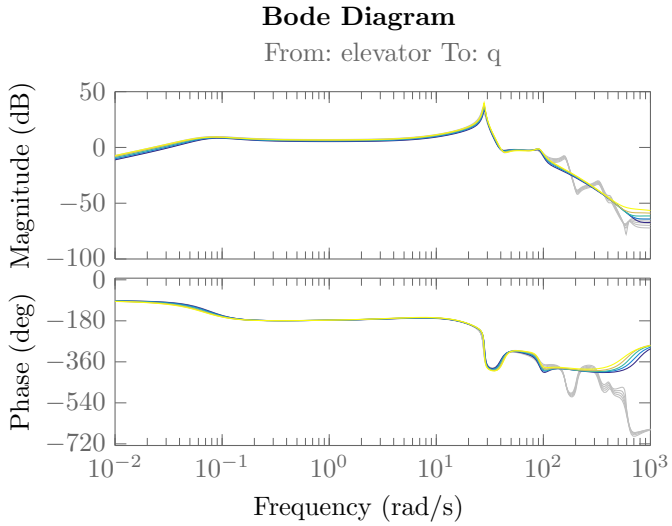

Fig. 7. Bode plots of the low and high fidelity (gray) models at $V = 25$ m/s.

In addition to comparing the low and high fidelity models, the parametric models are compared with the reference model of $\mu = 1$. The goal is to ensure that the models are not overly similar or too different from each other. Several options are available for such evaluation including ν-gap metrics, frequency response and baseline control examination. A detailed assessment on the effect of μ is presented in (Mocsanyi et al. (2019)). The current paper focuses on the ν-gap metric evaluation. Each parametric aircraft configuration is compared to the reference model at airspeeds between $V = [20, 33]$. To achieve better transparency, the maximum values are taken from the ν-gap values for the separate models. These maximum values are shown in Figure 8. It can be seen that the ν-gap values increase significantly, especially around the flutter frequency. This indicates that there is a sufficient difference between the parametric models and the attained parametric models can be applied for co-design.

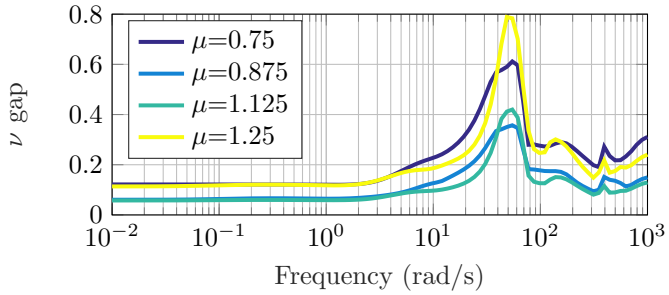

Fig. 8. ν-gap metrics of the parametric low fidelity model and the reference model.

6.2 TP type low fidelity LPV model of the mini MUTT

In addition to the grid based low fidelity LPV model, a TP type polytopic model is derived as well. The TP model transformation is applied to the grid based low fidelity LPV model taking the airspeed as the first varying parameter and μ as the second parameter. The highest resulting singular values in each dimension are

$$\sigma_{V_{ias}} = \begin{bmatrix} 1.19363e+07 \\ 7.12493e+04 \\ 49.843 \\ 1.0234 \\ 0.1049 \end{bmatrix}, \quad \sigma_{\mu} = \begin{bmatrix} 1.15341e+07 \\ 2.26827e+06 \\ 1.87955e+06 \\ 6.35425e+05 \\ 6.03685e+05 \end{bmatrix}$$

The singular values in the dimension of the airspeed drop significantly after the third singular value, thus only the first 3 singular values are kept in that dimension. However, the singular values that depend on μ have roughly similar magnitudes, thus, in that dimension no reduction is possible. Note, that since nonzero singular values are discarded, this is only an approximation of the grid-based LPV system. However, since the magnitude of the discarded singular values is small, the TP model provides a sufficiently accurate approximate model (Baranyi et al. (2013)). The vertexes of the polytopic model are given with system matrices $S^{3\times5\times51\times40}$. The weighting functions for the convex model is given in Figure 9.

As a result, a low fidelity grid-based and TP type parametric LPV models of the mini MUTT aircraft are available. The benefit of the TP type polytopic model compared to the grid based LPV model is that the synthesis can be done for the 3×5 vertex systems instead 27×5, which is the dimension of the grid based model. This leads to lower computational cost of the control synthesis. On the other hand, polytopic models inevitably include a certain degree of conservativeness. These two types of LPV models therefore complement each other and both can be investigated for co-design.

7. CONCLUSION

Grid-based and polytopic Co-design-compatible LPV models of the mini MUTT aircraft were developed. LPV models for the flexible aircraft model were obtained and reduced to a sufficiently low order using "bottom-up" modeling method. The ASE model is constructed via a subsystem based approach and defined utilizing the mean

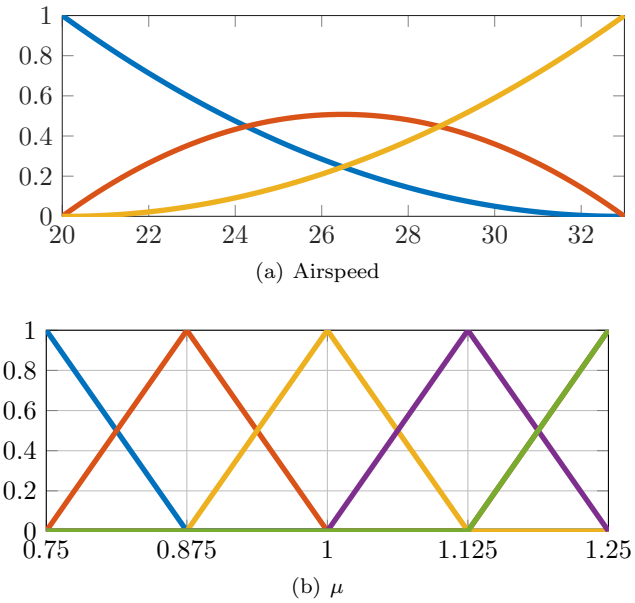

(a) Airspeed

(b) μ

Fig. 9. Weighting functions of the TP model.

axis constraints. This flexible model can be used for flutter suppression control synthesis. The resulting models were evaluated by Bode plot and ν-gap plot evaluations. It can be concluded that the resulting models show enough variations for the simultaneous control surface sizing and control synthesis optimization tasks, while not altering significantly the flutter characteristics. Future research steps are formulating the simultaneous optimization task as a Linear Fractional Representation (LFR) and to investigate the grid-based and TP type polytopic models in the co-design framework.

ACKNOWLEDGEMENTS

Innovációs és Technológiai Minisztérium

We would like to express our gratitude to the Aeroservoelastic Group at the University of Minnesota for providing us the access to the data used in this paper. The research leading to these results is part of the FLiPASED project. This project has received funding from the European Unions Horizon 2020 research and innovation programme under grant agreement No 815058. This paper was supported by the János Bolyai Research Scholarship of the Hungarian Academy of Sciences. The research reported in this paper was supported by the Higher Education Excellence Program of the Ministry of Human Capacities in the frame of Artificial Intelligence research area of Budapest University of Technology and Economics (BME FIKPMI/FM). Supported by the ÚNKP-19-4 New National Excellence Program of the Ministry for Innovation and Technology.

REFERENCES

AEM ASE (2013). University of minnesota, aeroeservoelastic group. `https://www.aem.umn.edu/ AeroServoElastic/`.

Apkarian, P., Gahinet, P., and Becker, G. (1995). Self-scheduled h∞ control of linear parameter-varying systems: a design example. *Automatica*, 31(9), 1251–1261.

Baranyi, P., Yam, Y., and Varlaki, P. (2013). *Tensor Product Model Transformation in Polytopic Model-Based Control*. CRC Press.

Denieul, Y., Bordeneuve-Guibé, J., Alazard, D., Toussaint, C., and Taquin, G. (2017). Integrated design of flight control surfaces and laws for new aircraft configurations. *IFAC-PapersOnLine*, 50(1), 14180–14187.

Deperrois, A. (2019). Xflr-5, open source vlm software.

FLEXOP (2015-2019). Flutter Free FLight Envelope eXpansion for ecOnomical Performance improvement (FLEXOP). Project of the European Union, Project ID: 636307.

FliPASED (2019-2022). Flight Phase Adaptive Aero-Servo-Elastic Aircraft Design Methods (FliPASED). Project of the European Union, Project ID: 815058.

Kotikalpudi, A. (2017). *Robust Flutter Analysis for Aeroservoelastic Systems*. Ph.D. thesis, University of Minnesota, Twin Cities.

L. Roger, K. (1977). Airplane math modelling methods for active control design. *AGARD Conf Proc*, 9.

Mocsanyi, R.D., Takarics, B., and Vanek, B. (2019). Grid-based lpv modeling of aeroelastic aircraft with parametrized control surface design. In *IEEE GPMC Control Conference*.

PAAW (2014-2019). Performance Adaptive Aeroelastic Wing Program. Supported by NASA NRA "Lightweight Adaptive Aeroelastic Wing for Enhanced Perfromace Across the Flight Envelope".

Packard, A. (1994). Gain scheduling via linear fractional transformations. *Systems & Control Letters*, 22(2), 79–92.

Regan, C.D. and Taylor, B.R. (2016). mAEWing1: Design, build, test - invited. In *AIAA Atmospheric Flight Mechanics Conference*. American Institute of Aeronautics and Astronautics.

Schmidt, D.K., Danowsky, B.P., Seiler, P.J., and Kapania, R.K. (2019). *Flight-Dynamics and Flutter Analysis and Control of an MDAO-Designed Flying-Wing Research Drone*. American Institute of Aeronautics and Astronautics.

Schmidt, D.K. (2011). *Modern Flight Dynamics*. McGraw-Hill Education.

Shamma, J.S. (1988). *Analysis and design of gain scheduled control systems*. Ph.D. thesis, Massachusetts Institute of Technology, Cambridge.

Takarics, B. and Seiler, P. (2015). Gain scheduling for nonlinear systems via integral quadratic constraints. In *2015 American Control Conference (ACC)*, 811–816.

Takarics, B., Vanek, B., Kotikalpudi, A., and Seiler, P. (2018). Flight control oriented bottom-up nonlinear modeling of aeroelastic vehicles. In *2018 IEEE Aerospace Conference*. IEEE.

Theis, J., Pfifer, H., and Seiler, P. (2016). Robust control design for active flutter suppression. *AIAA Science and Technology Forum and Exposition*.

Veenman, J. and Scherer, C.W. (2013). Stability analysis with integral quadratic constraints: A dissipativity based proof. 3770–3775. IEEE.

Vinnicombe, G. (1993). *Measuring robustness of feedback systems*. Ph.D. thesis, Univ. Cambridge, Cambridge.

Wu, F. (1995). *Control of Linear Parameter Varying Systems*. Ph.D. thesis, Univ. California, Berkeley.